

The assessment of the near infrared identification of carbon stars

I. The Local Group galaxies WLM, IC 10 and NGC 6822^{*,**}

P. Battinelli¹, S. Demers^{2,3}, and F. Mannucci³

¹ INAF, Osservatorio Astronomico di Roma, Viale del Parco Mellini 84, 00136 Roma, Italy
e-mail: battinell@oarhp1.rm.astro.it

² Département de Physique, Université de Montréal, C.P.6128, Succursale Centre-Ville, Montréal, Qc, H3C 3J7, Canada
e-mail: demers@astro.umontreal.ca

³ INAF - Istituto di Radioastronomia, Largo E. Fermi 5, 50125 Firenze, Italy
e-mail: filippo@arcetri.astro.it

Received 30 April 2007 / Accepted 18 July 2007

ABSTRACT

Context. The selection of AGB C and M stars from NIR colours has been done in recent years using adjustable criteria that are in needs of standardization if one wants to compare, in a coherent manner, properties of various populations.

Aims. We intend to assess the NIR colour technique to identify C and M stars.

Methods. We compare the NIR colours of several C stars previously identified from spectroscopy or narrow band techniques in WLM, IC 10 and NGC 6822.

Results. We demonstrate that very few M stars have $(J - K)_0 > 1.4$ but a non negligible number of C stars are bluer than this limit. Thus, counts of M and C stars based on such limit do not produce pure samples.

Conclusions. C/M ratios determined from NIR colours must be regarded as underestimates mainly because the M numbers include many warm C stars and also K stars if no blue limit is considered.

Key words. galaxies: individual: IC 10 – galaxies: individual: WLM – galaxies: individual: NGC 6822 – stars: carbon – stars: AGB and post-AGB – galaxies: dwarf

1. Introduction

Carbon stars were initially identified in large numbers by objective prism surveys, first in the Milky Way (Blanco 1965; Westerlund 1965) then a decade later similar surveys toward the Magellanic Clouds (Blanco et al. 1978) yielded hundreds of C stars. To reach fainter magnitudes, thus larger distances, a photometric technique based on two narrow band filters was introduced in the nineteen eighties (Richer et al. 1984; Cook et al. 1986). This approach, based on the (CN – TiO) index along with a colour, such as $(V - I)$ or $(R - I)$ has been successfully exploited to survey most of the Local Group galaxies (see for example: Battinelli & Demers 2005a; Brewer et al. 1995; Nowotny et al. 2003; Rowe et al. 2005). The narrow band technique presents, however, some serious drawbacks, the required filters are expensive to acquire and more importantly they are not available on major telescopes.

With the evolution of the near infrared (NIR) instrumentation Asymptotic Giant Branch (AGB) stars became the subjects of a number of observations in the Galaxy and beyond. Mould & Aaronson (1980) demonstrated that AGB stars in the SMC have slightly bluer NIR colours than their cousins in the LMC. Spectroscopically confirmed C stars were found to fall on an extend red tail in the $(J - K)$ vs. K plane, thus easily distinguishable

from the O-rich M stars. Survey of the literature reveals, however, that the C and M star border is ill-defined. Hughes & Wood (1990) found from their NIR survey of LMC Miras, with known spectral types, that 98% of O-rich stars have $(J - K) < 1.6$ while 15 out of 87 C-rich stars have $(J - K) < 1.6$. They therefore adopted a O- to C-rich transition at $(J - K) = 1.6$.

Davidge (2003) in his study of NGC 205 adopts, for C stars, $(J - K) > 1.5$ and $(H - K) > 0.4$ quoting Hughes & Wood (1990). Analyzing the 2MASS data for the LMC, Nikolaev & Weinberg (2000) set their blue limit of the C star region at $(J - K) \approx 1.4$. More recently, Cioni & Habing (2003) adopted $(J - K) > 1.4$ and $(J - K) > 1.3$ for the LMC and SMC, respectively. However, Cioni & Habing (2005) used another limit for the C stars in NGC 6822, namely $(J - K)_0 > 1.24$, while Kang et al. (2006) adopted for this galaxy $(J - K)_0 > 1.4$ and $(H - K)_0 > 0.45$. For NGC 147 Sohn et al. (2006) took $(J - K)_0 > 1.25$ and $(H - K)_0 > 0.41$ for the C stars identification. The same team used for NGC 185 the color limits $(J - K)_0 > 1.6$ and $(H - K)_0 > 0.48$ (Kang et al. 2005). Davidge (2005) chose $(J - K)_0 > 1.4$ and $(H - K)_0 > 0.45$ for both NGC 185 and NGC 147. Finally, Valcheva et al. (2007) assumed $(J - K)_0 > 1.20$ for the C stars in WLM. Several of the cited authors set the color limit inspecting the $(J - K)_0$ color histogram.

It is well known that the NIR colours of the RGB are function of the metallicity of the stellar population (Ferraro et al. 2000). The mean colours of O-rich or C-rich AGB stars brighter than the tip could similarly be metallicity dependent. There is at the present time no observational evidence for this effect. The NIR

* Based on observations obtained at the Italian Telescopio Nazionale Galileo.

** Full Tables 2 and 3 are only available in electronic form at <http://www.aanda.org>

colour comparison of the AGB in the Magellanic Clouds and a Galactic field (Schultheis et al. 2004) does not reveal such trend. From this brief literature survey it appears evident that, we are still far from any consensus about the use of NIR photometry to select C and M AGB stars. The different colour limits adopted are often introduced to account to some extent for metallicity differences of the parent galaxies. This could certainly explain why the published C/M ratios for a given galaxy sometime wildly differ.

In order to address this question we have started a program of *JHK* observations of several Local Group galaxies which already have a known C star population obtained from the (CN – TiO) index. The separation between O-rich and C-rich AGB stars based on the (CN – TiO) index has been proved (Brewer et al. 1996; Albert et al. 2000) to be very reliable as long as the optical colors of the stars are redder than a certain limit (e.g. $(R - I)_0 > 0.90$). For each galaxy, it is therefore reasonable to consider the sample of C stars identified with the narrow-band approach as a template to test other photometric criteria. In this first paper we discuss the case of three galaxies of different metallicities: WLM and IC 10 with newly acquired data, and NGC 6822 already available in the literature.

1.1. The target galaxies

Wolf-Lundmark-Melotte (WLM) dwarf galaxy is located on the periphery of the Local Group and it is seen at a high Galactic latitude ($\ell = 76^\circ, b = -74^\circ$), thus being essentially extinction free. From the investigation of Dolphin (2000), we adopt $(m - M)_0 = 24.90$ for its distance and a metallicity for its intermediate-age population of $[\text{Fe}/\text{H}] = -1.4$. WLM has been the target of a recent NIR study by Valcheva et al. (2007) who identified numerous C and M AGB stars. They determined a C/M ratio for WLM that is quite different from the one calculated by Battinelli & Demers (2004) from the (CN – TiO) criterion. As we shall see the difference comes mostly from the different sets of M and C stars.

IC 10 is a dwarf irregular galaxy, most probably associated with M31 and located at a rather low Galactic latitude ($\ell = 119^\circ, b = -3^\circ$). It is often described as the only starburst galaxy of the Local Group. Its study is hindered by the high reddening $E(B - V) \approx 0.8$ along the line of sight. IC 10 is not extremely metal poor, from the oxygen abundance of its HII regions Garnett (1990) determined $[\text{Fe}/\text{H}] = -0.8$, this value would correspond to its youngest population but intermediate-age stars should have slightly lower metallicities. The central star forming region of IC 10 has been observed in *JHK* by Borissova et al. (2000) who, however, did not comment on the presence of C stars. Since the starburst makes the central region difficult to investigate, our NICS observations target an outer region. IC 10 is particularly suited for NIR observations, it is relatively near at $(m - M)_0 = 24.35$, (Demers et al. 2004) and contains nearly 700 C stars distributed over an area much larger than its starburst core. From Demers et al. (2004) we have the *R*, *I* magnitudes of these C stars along with their narrow-band colors.

For NGC 6822 we will use the NIR photometry published by Kang et al. (2006) and the optical photometry by Letarte et al. (2002).

2. Colours of C stars

When looking at spectra it is quite easy to distinguish a late M star from a C star. From the photometric point of view, the

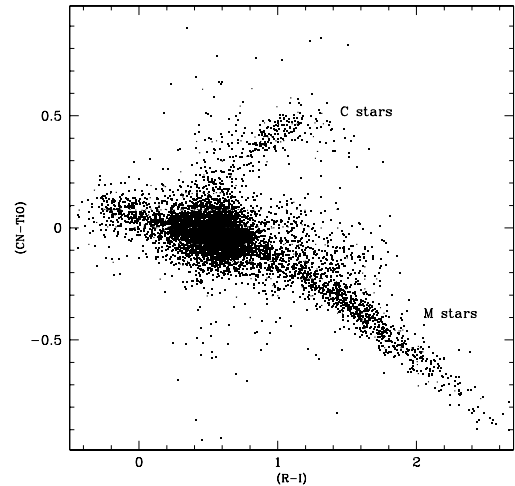


Fig. 1. A typical colour-colour diagram (WLM, Battinelli & Demers 2004) showing the C and M branches.

differences between the two types are not so clear cut. We believe that the best non-spectroscopic way to divide M and C stars is with the use of narrow band filters such as the (CN – TiO) index. A colour-colour diagram, based on this index and taken from Battinelli & Demers (2004) is shown in Fig. 1. The upper branch, corresponding to C stars is well isolated from the lower M star sequence. Investigation of the spatial distribution of the scattered points just above the M branch reveals that they corresponds to objects uniformly distributed over the CFH12K field. We believe that they are non-stellar objects with sharpness just below the rejection limit. A very informative figure showing the CN and TiO wavelength ranges over C and M spectra can be found in Nowotny et al. (2002). This technique has limitations however, it fails for bluer AGB stars, where the two branches converge into a big clump. In this particular example there are few blueish C stars but this is not always the case. For this reason we have adopted $(R - I)_0 = 0.90$ for the blue limit of the C and M star counts. Furthermore, there is no easy way to distinguish Galactic M dwarfs from giants without using time-consuming multicolor systems (e.g. Majewski et al. 2000).

Figure 2, taken from Demers et al. (2002), displays a near infrared colour-magnitude diagram of the spectroscopically identified C stars in the Large Magellanic Cloud. Figure 2 demonstrates that C stars, being distributed along the AGB, show an appreciable ($J - K$) colour range and also a large magnitude range. They are certainly not exclusively red. We also see that the use of C stars as standard candles requires a severe restriction on the selected colour range. Indeed, Weinberg & Nikolaev (2001), successfully used C stars selected in a *narrow colour range* as reliable standard candles to produce a 3D map of the LMC.

The study of NIR colours of spectroscopically identified C stars is unfortunately limited almost exclusively to the Magellanic Clouds. Indeed, many Galactic C stars have NIR colours but because the reddening in the plane is often far from negligible their observed colours are not so useful. Furthermore, to select C stars, one needs an unbiased colour selection not always achieved. This is certainly the case for the Fornax dwarf spheroidal galaxy where a few dozen C stars are known. Spectra of only the very red giants were obtained to confirm their C star nature (Mould & Aaronson 1980).

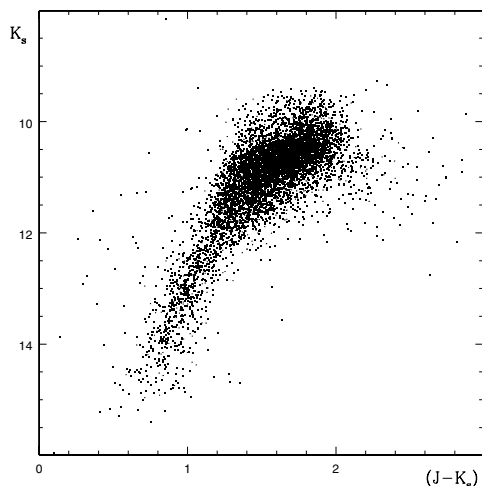


Fig. 2. The CMD of spectroscopically identified C stars in the LMC confirms their wide colour and magnitude ranges.

3. Observations and reduction

The J, H, K_p observations were secured with NICS (Near Infrared Camera Spectrometer; Baffa et al. 2001) installed at the Nasmyth focus of the TNG (Telescopio Nazionale Galileo) on the island of La Palma. NICS is based on a HgCdTe Hawaii 1024 \times 1024 array. The field of view for imaging is 4.2' \times 4.2'. One field in WLM 2.5' from its center and one 3' from the center of IC 10 were acquired with a 4 \times 4 dithering pattern. The central core of each galaxy is therefore excluded. Table 1 summarizes the observations obtained during two nights (IC 10: 2006-08-30; WLM: 2006-08-31) under photometric conditions with pretty stable seeing 0.7'' \div 0.8''. Data pre-reduction was performed with Speedy Near-infrared-data Automatic Pipeline (SNAP, Mannucci, in preparation), described in <http://www.tng.iac.es/news/2002/09/10/snap>. The basic steps of SNAP are briefly described here. After flat-fielding, a first-pass sky subtraction is performed and the resulting images are combined together. Objects detected in this image are masked out to perform a second-pass sky subtraction, improving the estimate of the sky level and the photometric accuracy. The final images are combined to a sub-pixel precision by cross-correlating the object masks.

The photometric reduction of the combined images is done by fitting model point-spread functions (PSFs) using DAOPHOT-II/ALLSTAR series of programs (Stetson 1987, 1994). Since the resulting images are medians, stars as bright as $K_s = 13.5$ are not saturated. Furthermore, we see no deviation from linearity when comparing the 2MASS magnitudes to the instrumental magnitudes of the IC 10 field.

4. Results

4.1. WLM

The line of sight toward WLM points far above the Galactic plane, thus our small field of view contains few Galactic stars but at faint magnitudes one would expect to detect more unresolved galaxies than stars. Cross identification with the 2MASS point source catalog yields only three matches brighter than $K_s < 14.6$,

Table 1. Journal of observations (J2000 coordinates).

Galaxy	RA	Dec	J	H	K_s
WLM	00:02:02	-15:30:00	3840 s	1280 s	1280 s
IC 10	00:19:55	+59:19:26	5760 s	1800 s	900 s

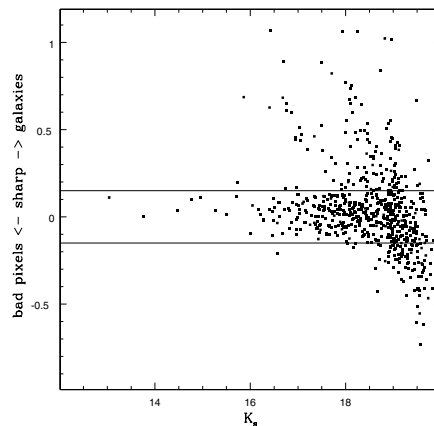


Fig. 3. SHARP distribution of the objects identifies in the three bands toward WLM. The two horizontal lines at ± 0.15 limit the region of stellar objects.

nevertheless a reliable calibration of our instrumental magnitudes is possible. We obtain the following zero point shifts:

$$K_s = -0.442(\pm 0.036) + K_{\text{inst}},$$

$$J = 1.010(\pm 0.060) + J_{\text{inst}},$$

$$H = 0.311(\pm 0.068) + H_{\text{inst}}.$$

DAOPHOT-II provides an image quality diagnostics SHARP. Stetson (1987) devises a sharpness criterion by comparing the height of the best-fitting Gaussian function to the height of a two-dimensional delta function, defined by taking the observed intensity difference between the central pixel of the presumed star image and the mean of the remaining pixels used in the fit. For isolated stars, SHARP should have a value close to zero, whereas for semi resolved galaxies and unrecognized blended doubles SHARP will be significantly greater than zero. On the other end, bad pixels and cosmic rays produce SHARP less than zero. SHARP must be interpreted as a function of the apparent magnitude of all objects because the SHARP parameter distribution degenerates near the magnitude limit; see Stetson & Harris (1998) for a discussion of this parameter. From Fig. 3 we define the stellar zone where SHARPs are within ± 0.15 from zero. The color-magnitude diagram (CMD) of the field in WLM is displayed in Fig. 4. Only stars with small SHARP parameters are plotted.

Table 2 lists the near infrared magnitude and colors of the 62 C stars previously identified. Magnitude errors are standard errors as defined by DAOPHOT thus not including the additional error from sky background variations. We note however that the calibrations of our instrumental magnitudes with 2MASS stars (particularly for IC 10 with 78 stars, next sub-section) yield calibration equations with slope 1 and dispersions along the trend of just a few hundreds of magnitudes thus suggesting a very efficient sky subtraction performed by SNAP. Colour errors are quadratic sums of the magnitude errors. Optical photometry and identification number are from Demers & Battinelli (2004).

Table 2. Known C stars in the WLM NICS field*.

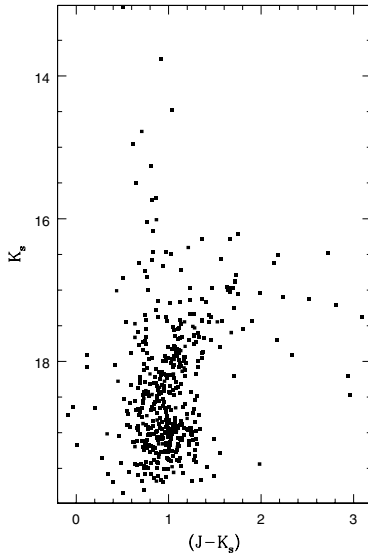
id	I	$(R - I)$	$(\text{CN} - \text{TiO})$	K_s	σ_K	$(J - K_s)$	σ_{JK}	$(H - K_s)$	σ_{HK}
23	20.404	1.233	0.833	17.428	0.061	1.904	0.064	0.731	0.068
24	20.142	1.532	0.387	16.795	0.043	1.730	0.048	0.609	0.052
26	20.260	1.026	0.477	17.729	0.076	1.293	0.077	0.362	0.080
29	20.230	1.083	0.486	17.428	0.063	1.364	0.065	0.347	0.066
31	20.145	0.965	0.405	17.885	0.104	1.114	0.108	0.154	0.112
38	20.238	0.971	0.363	17.665	0.086	1.147	0.088	0.239	0.090
41	19.956	1.218	0.458	17.446	0.073	1.526	0.077	0.476	0.083
43	19.995	0.931	0.451	17.531	0.063	1.281	0.065	0.285	0.068
44	20.373	1.000	0.454	17.937	0.087	1.178	0.090	0.268	0.092
45	21.104	1.128	0.446	17.255	0.051	1.703	0.053	0.549	0.055

* Table 2 is presented in its entirety in the electronic edition of *Astronomy & Astrophysics*. A portion is shown here for guidance regarding its form and content.

Table 3. Known C stars in the IC 10 NICS field*.

id	I_0	$(R - I)_0$	$(\text{CN} - \text{TiO})$	K_s	σ_K	$(J - K_s)$	σ_{JK}	$(H - K_s)$	σ_{HK}
51	20.085	0.911	0.531	17.036	0.051	2.220	0.055	0.831	0.072
58	19.306	1.193	0.373	16.494	0.032	2.089	0.037	0.713	0.038
60	19.571	1.194	0.512	16.720	0.038	2.067	0.043	0.752	0.045
62	20.092	0.985	0.518	17.247	0.051	1.989	0.055	0.694	0.062
63	20.186	1.037	0.530	17.147	0.047	2.247	0.053	0.762	0.058
68	19.651	0.900	0.410	17.237	0.056	1.732	0.061	0.552	0.067
70	20.183	1.203	0.638	16.879	0.041	2.533	0.046	1.052	0.051
71	19.253	0.992	0.687	16.606	0.032	2.039	0.036	0.717	0.039
73	20.213	1.088	0.480	16.900	0.039	2.234	0.043	0.853	0.049
75	19.662	0.963	0.671	17.362	0.062	1.770	0.065	0.524	0.068

* Table 3 is presented in its entirety in the electronic edition of *Astronomy & Astrophysics*. A portion is shown here for guidance regarding its form and content.

**Fig. 4.** CMD of WLM field.

4.2. IC 10

Thanks to its low Galactic latitude, the IC 10 NICS field contains 78 2MASS stars suitable for magnitude calibrations. We obtain the following zero points:

$$K_s = -0.264(\pm 0.032) + K_{\text{inst}},$$

$$J = 1.020(\pm 0.011) + J_{\text{inst}},$$

$$H = 0.299(\pm 0.022) + H_{\text{inst}}.$$

The CMD of the region observed in IC 10 is displayed in Fig. 5. We find in the NICS field 52 C stars, listed in Table 3, previously identified by Demers et al. (2004). According to our reddening map, the mean reddening in the NICS field is $E(B - V) = 0.86$ which corresponds following the relations of Schlegel et al. (1998) to $E(J - K) = 0.45$, $E(H - K) = 0.23$ and $A_K = 0.32$. The optical magnitudes and colours of IC 10 are individually deredden using our reddening map.

5. Discussion

To compare the NIR properties of C and M stars identified by the narrow-band technique, we show in the left panel of Fig. 6 an aspect of the cross-identification between our CFHT photometry of WLM (all stars) and our new NIR observations. We see two well separated groups of points: the C stars with $(\text{CN} - \text{TiO}) > 0.3$ and the K and M giants with negative $(\text{CN} - \text{TiO})$. The solid vertical line at $(J - K_s)_0 = 1.4$ is the often adopted limit for the C star selection (see Sect. 1). Stars with $(\text{CN} - \text{TiO})$ smaller than ≈ -0.3 have $(J - K_s)_0$ and $(H - K_s)_0$ colors typical of late dwarfs (see Bessell & Brett, 1988) that are seen here along the line of sight and mimic AGB stars. The dashed line is the Valcheva et al. (2007) limit to select C stars from the AGB stars found in their WLM study. They called AGB stars all the objects brighter than the TRGB. We must stress, however, that Valcheva et al. (2007) consider all the AGB stars bluer than $(J - K_s)_0 = 1.2$ as M stars. We see from Fig. 6 that their M star sample is certainly polluted by a number of C stars and certainly by stars earlier than spectral type M0. The right panel of Fig. 6. includes only C and M stars as defined from the RICNTiO photometry (Battinelli & Demers, 2004), i.e: C stars with $(\text{CN} - \text{TiO}) > 0.3$ and $(R - I)_0 > 0.9$ and M stars with $(\text{CN} - \text{TiO}) < 0$ and $(R - I)_0 > 0.9$. From the comparison of the two panels two facts emerge: 1) while the

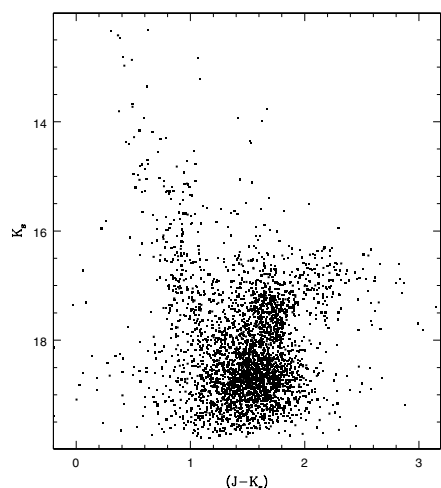


Fig. 5. CMD of IC 10 field.

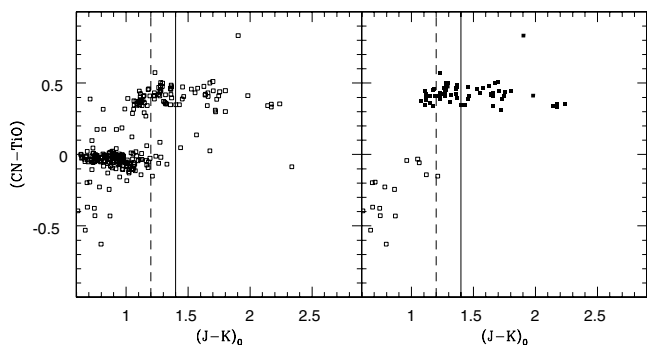


Fig. 6. *Left panel*: color-color plot of the WLM AGB stars seen in our NICS field. The two vertical lines correspond to the 1.2 and 1.4 $(J - K_s)_0$ limits. *Right panel*: C (filled squares) and M stars as defined from the RICNTiO photometry. In both panels only stars with K magnitudes brighter than the TRGB are plotted.

$(J - K_s)_0$ color threshold is appropriate as red limit for M stars it is not suitable for the blue limit of C stars. This limit implies that some C stars are misidentified as M-type; 2) the adoption of the $(R - I)_0 = 0.9$ threshold does not show a similar drawback, we see that nearly all the stars in the upper group are considered as C stars. On the other hand this limit cuts drastically the number of stars in the lower group. This is not surprising since stars with $(J - K)_0 < 1.0$ have spectral types earlier than M0 (Bessell & Brett 1988).

A similar plot, shown in Fig. 7, has been obtained for NGC 6822 by matching the published lists of C and M stars identified from NIR photometry by Kang et al. (2006) with Letarte et al. (2002) database. We see that for the stars in the upper group this galaxy behaves similarly to WLM. On the other hand, the adoption of the $(R - I)_0 = 0.9$ threshold does not cut seriously the number of stars in the bottom group, contrary to the case of WLM. This difference might very well be due to the higher metallicity of NGC 6822 that makes the RGB and AGB redder. This figure suggests $(J - K_s)_0 = 1.2$ as an appropriate limit for the C-M separation contrary to the $(J - K_s)_0 = 1.4$ adopted by Kang et al. (2006) on the basis of the color histogram. We notice the presence in the left panel of a number of red stars with $(CN - TiO) \approx 0$ that disappear in the right panel. These objects

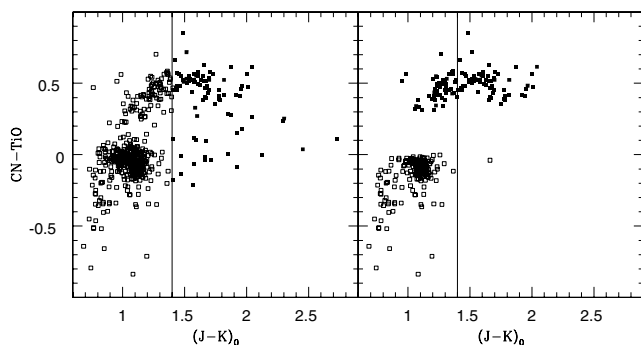


Fig. 7. *Left panel*: color-color plot of the M and C stars (filled squares) as defined by Kang et al. (2006) for NGC 6822. The vertical line correspond to the $(J - K_s)_0 = 1.4$ limit. *Right panel*: C (filled squares) and M stars as defined from the RICNTiO photometry.

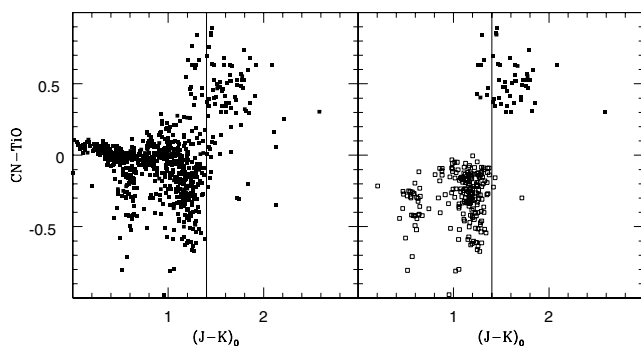


Fig. 8. Same as Fig. 6 for IC 10.

were therefore matched to stars with $(R - I)_0 < 0.9$. The easiest explanation for them is possible mismatches (within 1 arcsec). However a similar population is also visible in Fig. 1. From the spatial distribution of these odd objects we conclude they are background galaxies with sharpness small enough to mimic real stars.

Contrary to the two previous galaxies, nearly all C stars identified by the narrow band technique in IC 10 (see Fig. 8) have $(J - K_s)_0 > 1.4$. We see in this galaxy the presence of several objects with very negative $(CN - TiO)$. Such extreme negative $(CN - TiO)$ were already found in M 31 by Battinelli et al. (2003).

There is no doubt that numerous foreground red stars contribute to the large number of M stars seen in Fig. 8. As Demers et al. (2004) have shown, an accurate estimate of this foreground would be needed to properly determine the C/M ratio. We, however, do not need to know here this contribution since our aim is not to use our NIR to determine the C/M ratios but to assess the NIR approach.

We find in the literature three other Local Group galaxies which C star populations have been identified using NIR colors, namely NGC 147 (Sohn et al. 2006), NGC 185 (Kang et al. 2005) and NGC 205 (Davidge 2003). Unfortunately, the full lists of AGB stars in these galaxies are not available since the authors published no list or only the list of the identified C stars. There are no $(CN - TiO)$ observations of the Magellanic Cloud AGB stars.

We conclude, from what has been discussed above, that a color $(J - K_s)_0 = 1.4$ can be regarded as a conservative limit for the selection of C stars among the AGB stars. Indeed, stars

Table 4. Mean NIR properties of C stars with $\langle(J - K_s)_0\rangle > 1.4$.

Galaxy	[Fe/H]	N_C	$\langle K_{s,0}\rangle$	$\langle(J - K_s)_0\rangle$	$\langle(H - K_s)_0\rangle$	$\langle M_{K_s}\rangle$	$\langle R - J\rangle$	T_{eff}
LMC	-0.5	4617	10.59	1.65	0.56	-8.01		
IC 10	-0.8	212	16.77	1.74	0.57	-7.68	2.42	3400
NGC 147	-1.0	77	16.80	1.90	0.79	-7.60	2.67	3200
Fornax	-1.0	26	13.07	1.61	0.57	-7.67		
SMC	-1.1	317	11.18	1.62	0.58	-7.92		
NGC 6822	-1.25	141	15.85	1.77	0.75	-7.51	2.61	3250
NGC 185	-1.3	73	16.19	2.25	0.86	-7.93	0.17	?
WLM	-1.4	38	17.19	1.89	0.69	-7.71	2.39	3400

selected according to this criterion consist exclusively of C stars even though a non negligible number of genuine C stars, bluer than this adopted limit, may not be counted (depending on the metallicity). Another drawback of NIR colors compared to the narrow-band approach is the selection of AGB M stars. Beside the fact that a number of C stars are misidentified as M-type, very often all the stars above the TRGB and bluer than the above limit are considered as AGB M stars while obviously a blue $(J - K_s)_0$ color limit should be introduced to omit late K stars. The determination of such blue threshold is far from straightforward lacking a tight relation between $(J - K_s)_0$ colors and spectral types. The neglect of a blue limit to select AGB M stars led Valcheva et al. (2007) to largely overestimate the number of M stars. For instance, Valcheva et al. (2007) counted as M stars objects as blue as $(J - K_s)_0 = 0.5$ while such colour, according to Bessell & Brett (1988), corresponds to G2 giants. This obviously explains why their C/M ratio is much smaller than the value obtained by Battinelli & Demers (2004) using narrow band photometry. For all these reasons, C/M ratios deduced from the use of NIR colors significantly underestimate their real values.

Similar conclusions can be reached by comparing the $(H - K_s)_0$ colors of C and M stars. We found a $(H - K_s)_0 \approx 0.4$ limit is the counterpart of the $(J - K_s)_0 > 1.4$ even though not as clearly defined as the latter.

5.1. Mean NIR properties of C stars

In Table 4 we list the average NIR properties of the C stars identified in each galaxy by adopting the $(J - K_s)_0 > 1.4$ criterion for stars brighter than the TRGB. Distance moduli and [Fe/H] are from Battinelli & Demers (2005a). For WLM and IC 10, we determine the magnitude of the tip using the adopted [Fe/H] and the calibration published by Ivanov & Borissova (2002). Data for the LMC, SMC and Fornax are from Demers et al. (2002) while those for the other galaxies of from references cited above. The NGC 185 colours stand out as being quite red. A NIR survey of its AGB was done by Davidge (2005) who quotes a colour difference with Kang et al. (2005) of $\Delta(J - K_s) = 0.21$. We cannot cross identify Davidge's C stars with ours because their coordinates are not available.

In the last column we give the mean effective temperature calculated from Loidl et al. (2001) from the $\langle R - J\rangle$ of C stars. It is not too surprising that the C stars in each galaxy are very similar temperature wise. Only the redder stars, with $(J - K_s)_0 > 1.4$ are selected via the NIR approach. We note that the J magnitudes of C stars in NGC 185 as published by Kang et al. (2005) are too large making the $\langle R - J\rangle$ so small that no temperature can be calculated.

6. Conclusions

We have shown that the samples of C and M stars selected from NIR colors differ significantly from those obtained using the RICNTiO photometry. The main differences are:

- i) The NIR sample of M stars is polluted by a significant number of C stars misidentified as M. This is not the case for RICNTiO identified C stars where the $(\text{CN} - \text{TiO})$ color is an effective discriminant.
- ii) Both NIR and RICNTiO selection criteria for M stars require the adoption of a blue threshold to weed out K stars from the sample. In the RICNTiO approach, a limit of $(R - I)_0 = 0.9$ is generally adopted. Not all the authors using NIR color consider a similar blue limit, thus ending up with a large overestimate of the M star number.

Similarly, Groenewegen (2004), from a study of spectroscopically classified long period variables in the Magellanic Clouds, concludes that $(J - K) = 1.4$ cannot be used to properly separate M and C variables. From the above considerations it is evident that the C/M ratios obtained from NIR and narrow band photometry can be very different. It is therefore not justified to adopt C/M vs. [Fe/H] calibrations obtained from RICNTiO to convert NIR C/M into metallicities. A correct approach would be to calibrate the NIR C/M in terms of [Fe/H] similarly to what Battinelli & Demers (2005a) did for narrow band C/M.

On the basis of the data used in this paper the mean properties of C stars identified with NIR colors do not seem to be significantly sensitive to the metallicity of the parent galaxy. In particular, contrary to the $\langle M_I\rangle$ of C stars that has been proved to be fairly constant (Battinelli & Demers, 2005b), the $\langle M_{K_s}\rangle$ shows a wide range of variation.

Acknowledgements. This research is funded in parts (S.D.) by the Natural Sciences and Engineering Research Council of Canada. This publication makes use of data products from the Two Micron All Sky Survey, which is a joint project of the University of Massachusetts and the Infrared Processing and Analysis Center/California Institute of Technology, funded by the National Aeronautics and Space Administration and the National Science Foundation.

References

- Albert, L., Demers, S., & Kunkel, W. E. 2000, *AJ*, 119, 2780
 Baffa, C., Comoretto, G., Gennari, S., et al. 2001, *A&A*, 378, 722
 Battinelli, P., Demers, S., & Letarte, B. 2003, *AJ*, 125, 1298
 Battinelli, P., & Demers, S. 2004, *A&A*, 416, 111
 Battinelli, P., & Demers, S. 2005a, *A&A*, 434, 657
 Battinelli, P., & Demers, S. 2005b, *A&A*, 442, 159
 Bessell, M. S., & Brett, J. M. 1988, *PASP*, 100, 1134
 Blanco, V. M. 1965 in *Stars and Stellar Systems Vol. V*, ed. A. Blaauw and M. Schmidt (University of Chicago Press, Chicago), 241
 Blanco, B. M., Blanco, V. M., & McCarthy, M. F. 1978, *Nature*, 271, 638
 Borissova, J., Georgiev, L., Rosado, M., et al. 2000, *A&A*, 363, 130
 Brewer, J. P., Richer, H. B., & Crabtree, D. R. 1995, *AJ*, 109, 2480

- Brewer, J. P., Richer, H. B., & Crabtree, D. R. 1996, *AJ*, 112, 491
Cioni, M.-R. L., & Habing, H. J. 2003, *A&A*, 402, 133
Cioni, M.-R. L., & Habing, H. J. 2005, *A&A*, 429, 837
Cook, K. H., Aaronson, M., & Norris, J. 1986, *ApJ*, 305, 634
Davidge, T. J. 2003, *ApJ*, 597, 289
Davidge, T. J. 2005, *AJ*, 130, 2087
Demers, S., Dallaire, M., & Battinelli, P. 2002, *AJ*, 123, 3428
Demers, S., Battinelli, P., & Letarte, B. 2004, *A&A*, 424, 125
Dolphin, A. E. 2000, *ApJ*, 531, 804
Ferraro, F. R., Montegriffo, P. A., & Fusi-Peccì, F. 2000, *AJ*, 119, 1282
Garnett, D. R. 1990, *ApJ*, 363, 142
Groenewegen, M. A. T. 2004, *A&A*, 425, 595
Hughes, S. M. G., & Wood, P. R. 1990, *AJ*, 99, 784
Ivanov, V. D., & Borissova, J. 2002, *A&A*, 390, 937
Kang, A., Sohn, Y.-J., Rhee, J., et al. 2005, *A&A*, 437, 61
Kang, A., Sohn, Y.-J., Kim, H.-L., et al. 2006, *A&A*, 454, 717
Letarte, B., Demers, S., Battinelli, P., & Kunkel, W. E. 2002, *AJ*, 123, 832
Loidl, R., Lançon, A., & Jørgensen, U. G. 2001, *A&A*, 371, 1065
Majewski, S. R., Ostheimer, J. C., Patterson, R. J., et al. 2000, *AJ*, 119, 760
Mould, J., & Aaronson, M. 1980, *ApJ*, 240, 464
Nikolaev, S., & Weinberg, M. D. 2000, *ApJ*, 542, 804
Nowotny, W., & Kirschbaum, F. 2002, *Hvar Obs. Bull.*, 26, 63
Nowotny, A., Kerschbaum, F., Olofsson, H., & Schwarz, H. E. 2003, *A&A*, 403, 93
Rowe, J., Richer, H., Brewer, J., & Crabtree, D. 2005, *AJ*, 129, 729
Richer, H. B., Crabtree D. R., & Pritchett, C. J. 1984, *ApJ*, 287, 138
Schlegel, D., Finkbeiner, D., & Davis, M. 1998, *ApJ*, 500, 525
Schultheis, M., Glass, I. S., & Cioni, M.-R. 2004, *A&A*, 427, 945
Sohn, Y.-J., Kang, A., Rhee, J., et al. 2006, *A&A*, 445, 69
Stetson, P. B. 1987, *PASP*, 99, 191
Stetson, P. B. 1994, *PASP*, 106, 250
Stetson, P. B., & Harris, W. E. 1988, *AJ*, 96, 909
Valcheva, A. T., Ivanov, V. D., Ovcharov, E. P., & Nedialkov, P. L. 2007, *A&A*, 466, 501
Weinberg, M. D., & Nikolaev, S. 2001, *ApJ*, 548, 712
Westerlund, B. E. 1965, *MNRAS*, 130, 45

Online Material

Table 2. Known C stars in the WLM NICS field.

Id	I	$(R - I)$	$(\text{CN} - \text{TiO})$	K_s	σ_K	$(J - K_s)$	σ_{JK}	$(H - K_s)$	σ_{HK}
23	20.404	1.233	0.833	17.428	0.061	1.904	0.064	0.731	0.068
24	20.142	1.532	0.387	16.795	0.043	1.730	0.048	0.609	0.052
26	20.260	1.026	0.477	17.729	0.076	1.293	0.077	0.362	0.080
29	20.230	1.083	0.486	17.428	0.063	1.364	0.065	0.347	0.066
31	20.145	0.965	0.405	17.885	0.104	1.114	0.108	0.154	0.112
38	20.238	0.971	0.363	17.665	0.086	1.147	0.088	0.239	0.090
41	19.956	1.218	0.458	17.446	0.073	1.526	0.077	0.476	0.083
43	19.995	0.931	0.451	17.531	0.063	1.281	0.065	0.285	0.068
44	20.373	1.000	0.454	17.937	0.087	1.178	0.090	0.268	0.092
45	21.104	1.128	0.446	17.255	0.051	1.703	0.053	0.549	0.055
47	20.746	1.553	0.410	17.055	0.042	1.747	0.045	0.592	0.045
50	21.078	1.241	0.420	17.955	0.101	1.362	0.102	0.394	0.105
58	20.161	1.317	0.511	16.977	0.039	1.700	0.042	0.553	0.044
59	20.226	1.002	0.469	17.510	0.064	1.262	0.065	0.302	0.069
60	20.283	0.982	0.420	17.510	0.064	1.262	0.065	0.302	0.069
62	19.642	1.389	0.439	16.210	0.019	1.755	0.021	0.601	0.025
63	20.003	0.986	0.343	17.446	0.070	1.171	0.071	0.216	0.072
65	20.308	1.139	0.463	17.416	0.058	1.357	0.060	0.350	0.062
70	19.835	0.921	0.349	17.447	0.061	1.431	0.063	0.444	0.065
71	20.000	1.098	0.427	17.535	0.070	1.116	0.077	0.250	0.072
72	20.420	1.146	0.473	17.379	0.054	1.456	0.056	0.450	0.059
72	20.420	1.146	0.473	17.971	0.099	1.059	0.102	0.145	0.104
73	20.023	1.041	0.355	17.096	0.045	2.239	0.050	0.924	0.052
74	20.137	1.272	0.310	16.890	0.036	1.720	0.039	0.562	0.040
75	19.581	1.068	0.432	16.286	0.024	1.660	0.026	0.510	0.030
76	20.155	1.053	0.349	17.170	0.047	1.401	0.050	0.369	0.051
77	20.212	1.106	0.474	17.121	0.043	1.366	0.045	0.335	0.046
78	20.848	1.118	0.504	17.764	0.076	1.278	0.077	0.360	0.080
82	20.252	1.146	0.573	17.137	0.043	1.233	0.044	0.267	0.048
83	20.237	1.011	0.440	17.647	0.075	1.275	0.077	0.378	0.079
84	20.231	0.991	0.438	17.647	0.075	1.275	0.077	0.378	0.079
85	20.034	1.051	0.419	17.603	0.072	1.317	0.075	0.335	0.077
86	20.207	1.658	0.352	17.696	0.073	2.172	0.079	0.883	0.081
88	20.257	1.510	0.333	17.696	0.073	2.172	0.079	0.883	0.081
90	20.131	0.926	0.444	17.691	0.072	1.106	0.074	0.231	0.075
91	20.121	1.051	0.410	17.696	0.087	1.224	0.088	0.310	0.094
92	20.071	1.238	0.501	17.597	0.130	1.676	0.134	1.411	0.173
93	19.591	1.049	0.432	16.965	0.042	1.228	0.045	0.322	0.046
94	19.636	0.952	0.413	16.965	0.042	1.228	0.045	0.322	0.046
95	20.134	0.987	0.388	17.699	0.085	1.453	0.091	0.402	0.093
98	20.444	0.926	0.411	17.336	0.053	1.272	0.054	0.350	0.055
101	20.010	1.237	0.417	17.001	0.042	1.638	0.045	0.518	0.045
103	19.868	1.151	0.407	16.974	0.038	1.465	0.039	0.390	0.041
105	19.016	1.069	0.457	16.277	0.023	1.362	0.025	0.339	0.026
106	20.104	1.039	0.396	17.872	0.086	1.367	0.091	0.344	0.090
107	19.938	1.257	0.407	17.023	0.041	1.661	0.044	0.499	0.044
111	20.834	1.061	0.499	18.170	0.105	1.294	0.108	0.281	0.110
112	20.427	1.329	0.464	17.436	0.060	1.577	0.062	0.433	0.065
113	20.538	1.058	0.410	18.023	0.112	1.191	0.114	0.211	0.116
119	20.000	1.286	0.477	16.960	0.043	1.628	0.044	0.531	0.046
120	20.709	1.410	0.343	16.614	0.029	2.142	0.033	0.837	0.033
121	19.903	1.193	0.422	17.003	0.039	1.639	0.042	0.525	0.043
124	20.310	1.399	0.343	16.966	0.046	1.655	0.049	0.518	0.049
127	20.414	1.134	0.447	17.549	0.070	1.801	0.075	0.584	0.075
131	20.427	1.000	0.477	17.628	0.073	1.276	0.074	0.302	0.076
132	20.497	0.935	0.481	17.628	0.073	1.276	0.074	0.302	0.076
133	20.264	0.916	0.365	17.989	0.102	1.313	0.104	0.317	0.106
134	19.777	1.162	0.412	17.037	0.049	1.982	0.053	0.692	0.058
134	19.777	1.162	0.412	18.140	0.123	1.146	0.125	0.261	0.129
139	20.383	1.118	0.433	17.797	0.078	1.556	0.080	0.459	0.083
140	20.536	1.033	0.459	18.206	0.131	1.182	0.135	0.232	0.142
146	20.215	1.043	0.389	17.342	0.066	1.229	0.069	0.267	0.073

Table 3. Known C stars in the IC 10 NICS field.

Id	I_0	$(R - I)_0$	(CN - TiO)	K_s	σ_K	$(J - K_s)$	σ_{JK}	$(H - K_s)$	σ_{HK}
51	20.085	0.911	0.531	17.036	0.051	2.220	0.055	0.831	0.072
58	19.306	1.193	0.373	16.494	0.032	2.089	0.037	0.713	0.038
60	19.571	1.194	0.512	16.720	0.038	2.067	0.043	0.752	0.045
62	20.092	0.985	0.518	17.247	0.051	1.989	0.055	0.694	0.062
63	20.186	1.037	0.530	17.147	0.047	2.247	0.053	0.762	0.058
68	19.651	0.900	0.410	17.237	0.056	1.732	0.061	0.552	0.067
70	20.183	1.203	0.638	16.879	0.041	2.533	0.046	1.052	0.051
71	19.253	0.992	0.687	16.606	0.032	2.039	0.036	0.717	0.039
73	20.213	1.088	0.480	16.900	0.039	2.234	0.043	0.853	0.049
75	19.662	0.963	0.671	17.362	0.062	1.770	0.065	0.524	0.068
76	19.628	1.266	0.317	16.579	0.032	2.270	0.037	0.886	0.041
78	19.999	1.126	0.486	17.124	0.046	1.992	0.050	0.674	0.060
83	19.529	1.539	0.531	16.614	0.054	2.224	0.075	0.993	0.073
88	19.496	0.919	0.410	16.821	0.046	1.928	0.056	0.592	0.056
92	19.963	0.987	0.455	17.165	0.054	2.011	0.066	0.678	0.066
98	19.799	1.130	0.641	16.777	0.038	2.094	0.044	0.833	0.049
101	19.945	0.934	0.704	17.142	0.052	1.860	0.055	0.649	0.062
104	20.118	1.247	0.392	17.162	0.055	2.158	0.060	0.676	0.065
108	19.911	1.374	0.301	16.895	0.038	2.317	0.044	0.887	0.050
109	20.095	1.018	0.847	17.671	0.080	1.752	0.085	0.597	0.093
110	19.541	1.282	0.643	16.852	0.036	1.913	0.039	0.641	0.042
111	19.792	0.985	0.639	16.806	0.037	1.740	0.041	0.555	0.044
114	19.788	0.984	0.526	16.998	0.048	2.093	0.051	0.739	0.060
116	19.887	0.955	0.310	17.819	0.112	3.034	0.163	1.254	0.157
117	19.392	1.219	0.524	16.628	0.040	2.108	0.049	0.772	0.051
121	19.850	0.908	0.501	17.014	0.049	2.165	0.056	0.827	0.059
124	19.674	1.256	0.474	17.246	0.060	1.808	0.070	0.538	0.069
125	19.888	1.481	0.538	16.452	0.026	2.223	0.031	0.807	0.033
126	19.472	0.929	0.638	16.731	0.037	2.370	0.044	0.895	0.052
126	19.472	0.929	0.638	16.806	0.041	2.032	0.044	0.695	0.051
127	19.585	1.229	0.647	16.731	0.037	2.370	0.044	0.895	0.052
129	20.136	1.021	0.530	17.820	0.096	1.927	0.102	0.640	0.110
131	19.499	1.125	0.639	16.730	0.033	1.701	0.075	0.606	0.051
132	19.794	1.124	0.850	17.104	0.053	1.899	0.077	0.643	0.064
135	19.341	1.007	0.474	16.799	0.035	1.964	0.039	0.704	0.043
143	19.701	1.159	0.773	16.631	0.044	1.701	0.084	0.719	0.055
145	19.627	1.102	0.308	16.689	0.033	2.055	0.045	0.680	0.045
149	19.336	1.265	0.741	16.315	0.028	2.242	0.043	0.939	0.041
151	19.720	1.369	0.606	16.603	0.040	2.827	0.094	1.054	0.068
156	19.791	1.102	0.627	17.411	0.070	2.098	0.082	0.752	0.084
161	18.981	1.051	0.415	16.369	0.032	2.154	0.049	0.863	0.053
165	19.355	1.189	0.353	16.610	0.044	2.015	0.063	0.681	0.061
167	19.098	1.601	0.487	16.484	0.038	1.973	0.052	0.708	0.047
168	19.494	1.487	0.614	16.579	0.037	1.991	0.049	0.698	0.046
175	19.711	1.209	0.631	16.792	0.042	2.121	0.055	0.837	0.057
176	18.978	1.481	0.301	15.938	0.019	2.299	0.032	0.791	0.025
189	19.086	1.116	0.566	16.446	0.039	2.094	0.056	0.698	0.046
191	19.427	1.478	0.532	16.294	0.032	2.175	0.052	0.759	0.050
193	19.670	1.413	0.625	16.349	0.026	1.963	0.032	0.737	0.035
195	19.371	1.289	0.559	16.358	0.025	2.225	0.030	0.764	0.035
197	19.768	1.163	0.307	16.987	0.057	2.002	0.073	0.705	0.084
198	18.894	1.058	0.429	16.451	0.043	1.804	0.051	0.573	0.055